

Effect of molecular weight blending on the fracture energy and morphology of the semicrystalline polymer poly(1,4-dimethylene-*trans*-cyclohexyl seberate)

J. M. Pochan,* W. F. Parsons, J. F. Elman and R. O. Gutierrez

Research Laboratories, Eastman Kodak Company, Rochester, New York 14650, USA

(Received 5 July 1985; revised 24 January 1986)

Fracture studies were made on bimodal molecular weight blends of poly(1,4-dimethylene-cyclohexyl seberate) (MCS), where small additions of low-molecular polymer to the higher molecular weight material drastically decreased the crack propagation energy. The data are rationalized in terms of exclusion of the low-molecular weight fraction from the crystalline matrix during crystallization. These blends have a unique minimization of spherulite size as a function of composition. This effect is explained in terms of changes of surface free energy of crystal nuclei as a function of molecular weight. Fracture morphology shows almost total brittle fracture of the blends. This result corresponds to the drastic decrease in propagation energy in these blends and suggests that most of the data showing a high propagation energy are due to plastic deformation. The temperature dependence of the energy to propagate a crack, G_p , is explained in terms of a local-deformation (thermally activated) model. The activation energies obtained, as a function of blending and annealing conditions, are discussed in terms of linear damage theory.

(Keywords: morphology; fracture energy; poly(1,4-dimethylene seberate); crack propagation)

INTRODUCTION

Recently we reported on the effects of morphology and temperature on the fracture parameters of the semicrystalline polymer poly(1,4-dimethylene-*trans*-cyclohexyl seberate) (MCS)^{1,2}. We showed that (1) the degree of crystallinity of the polymer varied little from $45 \pm 3\%$ with various annealing and forming temperatures, (2) ambient fracture energy was directly correlated with the impingement spherulitic size, and (3) a simplified local flow model could be used to explain the temperature dependence of the energy to propagate a crack (G_p) of various formed morphologies. These studies were made on MCS of two molecular weights, $M_n = 25$ K, $MWD = 1.92$ (MCS-I) and $M_n = 38$ K, $MWD = 2.55$ (MCS-II).

Fracture morphologies for the polymers varied from pure interspherulitic failure to total plastic deformation with increasing molecular weight. We showed earlier² that a modified Griffith criterion, similar to that used by Bentle and Kniefel³ in a study of ceramic fracture, could be used to describe MCS failure. Those results provide a $G_p \sim R^{-1/2}$ correlation, indicating grain-boundary failure. Similar results were observed for MCS, indicating interspherulitic failure¹. The results were rationalized in terms of weak interspherulitic boundary layers caused by molecular weight redistribution during isothermal crystallization⁴. This behaviour suggests that molecular weight can be an important parameter in determining the fracture properties of semicrystalline materials. The

following study was thus undertaken to ascertain the effect of molecular weight blending on the fracture parameters of MCS.

EXPERIMENTAL

Physical characterization

Figure 1 shows the chemical structure of MCS. Figure 2 shows a micrograph indicating that MCS exists in a banded spherulite conformation. Two molecular weight samples were used in this study: MCS-I and MCS-III ($M_n = 8.8$ K, $M_w = 16$ K). (MCS-III is designated for consistency with our earlier publications^{1,2}.) MCS-I is above the entanglement molecular weight, and MCS-III is in the $S = 1-3.4$ transition zone on a log-log plot of zero shear viscosity vs. molecular weight. Polymer crystallinity determined via d.s.c. varied slightly with temperature of formation from the melt but can be considered constant at $45 \pm 3\%$. This suggests little effect of the degree of crystallinity on the observed mechanical properties of the polymer⁶. Annealing has also been shown to have little effect on the degree of crystallinity of MCS. T_m for all samples tested was $\sim 97^\circ\text{C}$, and T_g was below ambient. Lamellar thickening has been noted in samples annealed above 90°C ^{1,7}. Impingement spherulite size was determined via small-angle light scattering⁸. All samples exhibit banding morphology that changes character above 85°C ¹. Band size was determined via secondary light scattering⁹.

Sample preparation

Weight-percent blends were made by dissolving appropriate amounts of MCS-I and -III in

* Author to whom correspondence should be addressed. Present address: S. C. Johnson and Son, Racine, WI 53403-5011, USA.

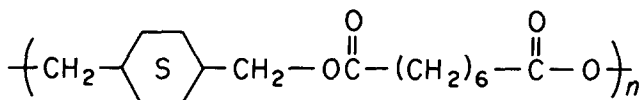


Figure 1 Chemical structure of poly(1,4-dimethylene-trans-cyclohexyl seberate)

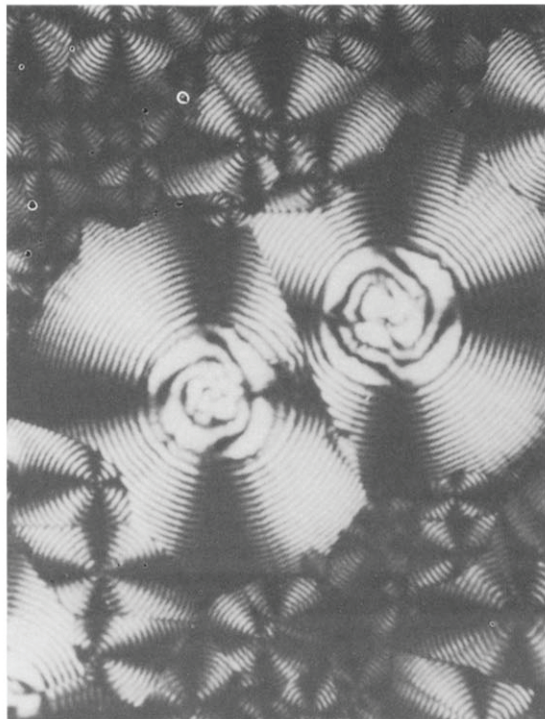


Figure 2 Spherulitic morphology of MCS. Magnification ~400x

tetrahydrofuran (THF) with stirring at ~65°C. The solutions was poured onto a Teflon[®] surface, and the THF evaporated at ambient. The THF was completely removed by melting the blends at 120°C in a vacuum oven. The blend was allowed to cool and cut into strips that could fit into a 1 × 10 × 0.32 cm mould. Silicone rubber 0.32 cm thick was used to form the sides and ends of the moulds, and 3-mil Teflon[®]-coated Kapton (Du Pont) formed the base of the mould. The whole assembly rested on a 1/16-in-thick stainless steel plate. Cracks were produced in the samples by moulding a sheet of 3 mm Teflon-coated Kapton (TKT) into the sample. This material was fitted into a cut in the silicone rubber and extended 0.5 cm into the mould cavity. The blend was melted in the mould cavity at 120°C, and while the blend was molten, a second piece of 3 mm TKT was placed in contact with the top side of the molten blend and covered with a 1/16 inch thick piece of stainless steel, also at 120°C. This assembly was quenched in water at the appropriate temperature and annealed for 21 h in a circulating-air oven. After annealing, the sample was removed from the mould, and the TKT that formed the crack was pulled from the sample. The crack structure was thus well annealed.

Mechanical testing

Crack propagation was studied on an Instron model 1113 instrument. Samples were held in pneumatic grips and tested in tension. The gauge length for all samples was 4.5 cm. The crack tip was observed with a Gaertner optical extensometer, and propagation was noted

visually. The crosshead rate for these experiments was 0.2 cm/min.

Samples tested at high temperature were equilibrated for ~20 min before loading and crack propagation. The sample was assumed to be at equilibrium when no forces developed in the Instron due to thermal expansion of the sample. Within the 20 min equilibration, lamellar thickness is not expected to vary significantly for those samples formed at low temperature and tested at a higher temperature¹⁰. Four experimental temperatures were chosen for propagation studies: 23°C, 55°C, 72°C and 90°C. Mechanical data such as energy-to-break were calculated in the standard fashion^{1,2}.

RESULTS AND DISCUSSION

Morphology

Plots of spherulitic size and band size versus forming temperature are shown in Figures 3 and 4. Both exhibit a minimum as a function of composition. The minimum is more pronounced at higher annealing temperatures. All the data can be fit with an equation of the form:

$$\bar{R} = W_1 R_1 + W_2 R_2 + A W_1 W_2 \quad (1)$$

where R_i is the measured impingement radius of the pure

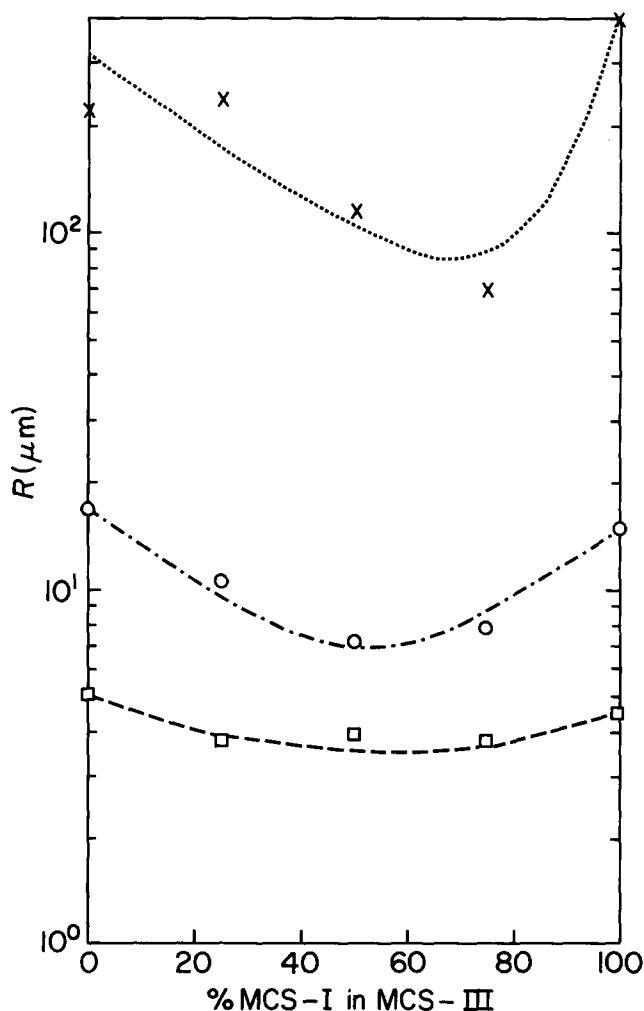


Figure 3 Impingement spherulite size versus weight per cent MCS-I in an MCS-I/MCS-III mixture. Forming temperatures: (□) 23°C, (○) 55°C, (×) 85°C

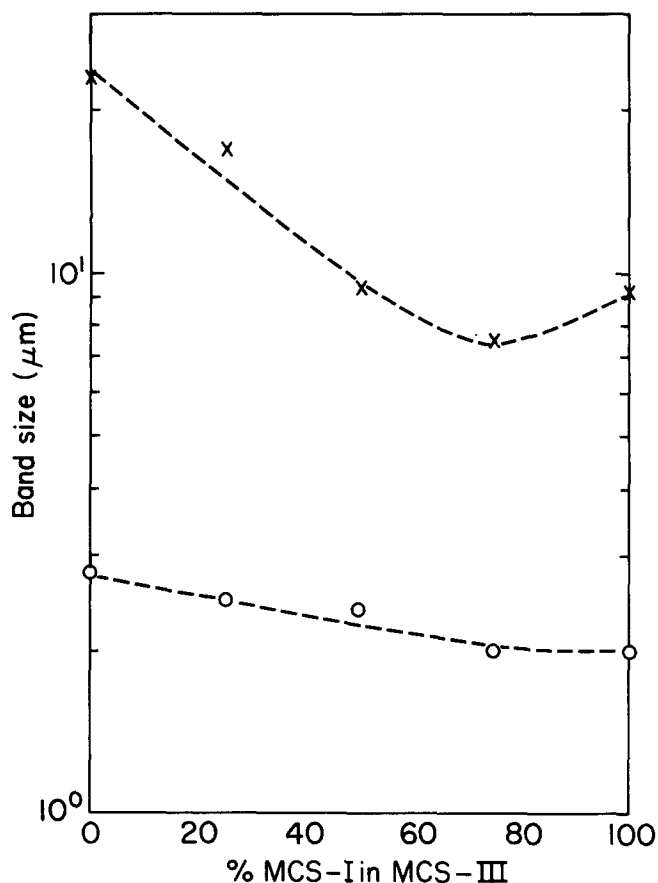


Figure 4 Spherulitic band size versus weight per cent MCS-I in an MCS-I/MCS-III mixture. Forming temperatures: (○) 55°C, (×) 85°C

molecular weight samples used, and W_i is the weight fraction of each component. A fit of the 55°C data is shown in Figure 3 with $R(\text{MCS-I})=15\ \mu\text{m}$, $R(\text{MCS-III})=17\ \mu\text{m}$, and $A=-36$. The fit is good and may indicate an interactive control of the observed morphology.

How can such data be rationalized? These results suggest that the addition of either component to the other affects nucleation and growth such that the average spherulitic size becomes smaller. Earlier work has shown a molecular weight dependence of crystalline growth rate^{4,5}. For silane-based polymers, this rate was proportional to $M^{-1/2}$.⁵ Growth rate studies on MCS¹ suggest almost an M^{-1} dependence. The $M^{-1/2}$ and M^{-1} dependences predict a monotonic trend of spherulite size as molecular weight composition changes but this is not observed.

Growth rates of a blend and pure MCS-I and -III have been studied. The growth kinetics for these materials are essentially linear from nucleation to impingement, showing that the impurity segregation (i.e. a gradual build up of low-molecular weight impurity at the crystalline growth front) proposed by Keith and Padden^{11,12} does not occur in this system. Figure 5 is a plot of growth rate versus composition for the blends. At the two temperatures tested, the growth rate varies monotonically with composition and has no maximum or minimum as observed for the spherulitic-size plot. The data also show that decreasing molecular weight increases the growth rate, as observed in many polymeric systems. Because of these facts, it is tempting to assign the above behaviour to a nucleation phenomenon.

Nucleation rates are a function of free energy of formation and the microviscosity of the nucleating system¹⁰:

$$\dot{N} = \dot{N}_0 e^{-\Delta F/RT} e^{-\Delta E_a/RT} \quad (2)$$

where ΔF is the free energy of nuclei formation, and E_a is the activation energy for viscous flow. Equation (2) predicts that nucleation rate should go through a maximum as a function of temperature below T_m , with the free energy term driving nucleation near T_m and the viscosity term controlling large supercooling values. ΔF can be derived in terms of a surface free energy of the nucleus (σ), the heat of fusion of a 100% crystalline material (ΔH_f) and the degree of supercooling of the melt ($\Delta T = T_m - T$)

$$\Delta F = \frac{C\sigma^3 T_m^2}{\Delta H_f^2 R \Delta T^2} \quad (3)$$

where T_m is the melting point of the material. Equation (3) is obtained by assuming a nuclear shape and minimizing the free energy as a function of size⁴. The data on MCS can be rationalized as being caused by the bimodal distribution of polymer causing equation (3) to be affected in such a way as to increase nucleation rate in the intermediate composition range. This effect appears to have been caused by changes in σ , as the degree of crystallinity for all blends at a given annealing condition is invariant as measured via d.s.c. This effect on σ could be caused by microphase separation of MCS of various

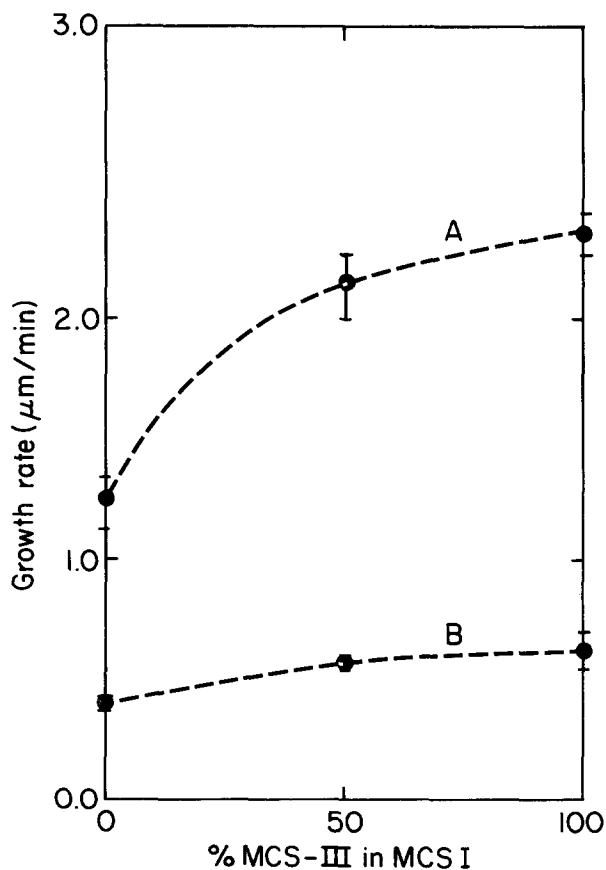


Figure 5 Growth rate versus composition for blends of MCS-I and MCS-III as a function of composition and temperature (A, 80°C; B, 85°C)

molecular weights during crystallization, i.e. the rejection of low-molecular weight material from the growing nucleus. Such an effect would become more dominant in the intermediate composition range and could be considered entropic.

Energy to crack propagation and other mechanical properties

The modulus of MCS as a function of composition and experimental temperatures has been ascertained. The general trend is that for a given forming temperature, Young's modulus decreases with increasing test temperature and decreases with increasing MCS-I concentration. All values were, however, within a factor of 6 of one another and only average values are listed in Table 1. Within limits of error, all values are identical, showing that the degree of crystallinity of all these samples is relatively constant⁶.

The initial purpose of this study was to ascertain the effect of addition of low-molecular weight MCS to high molecular-weight material. If our original postulate concerning separation by molecular weight during crystallization is correct, addition of small amounts of the weaker MCS-III to the tougher MCS-I should weaken MCS-I. Such an effect is dramatically shown in Figure 6;

Table 1 Young's modulus as a function of forming temperature

Forming temperature (°C)	$E \times 10^6$
23	2.54 ± 1.48
55	2.21 ± 1.00
85	2.40 ± 1.23

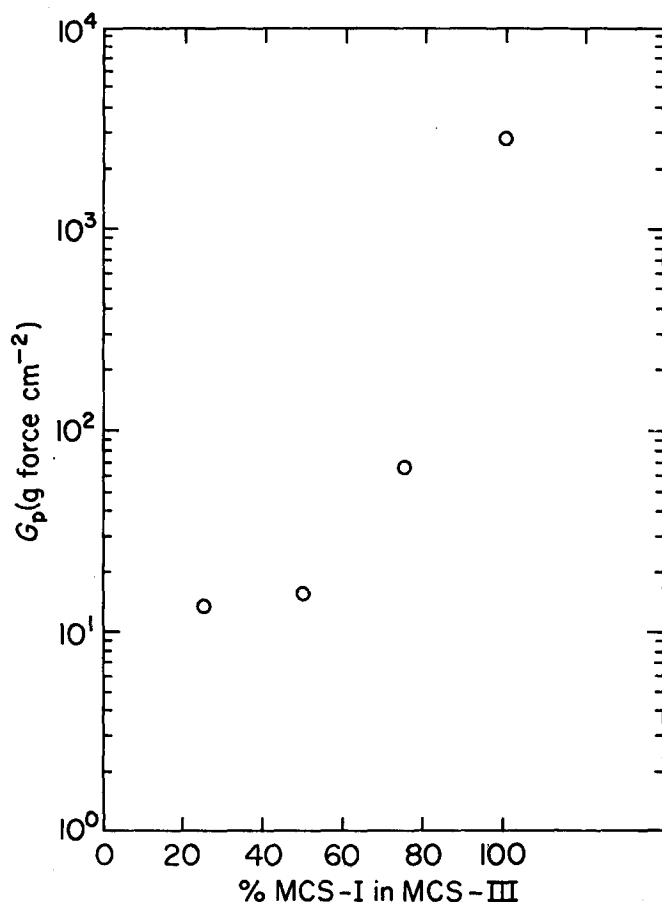


Figure 6 Energy to propagate versus weight per cent MCS-I in MCS-III. Forming temperature 23°C

the addition of 20% MCS-III to MCS-I lowered the energy to propagate a crack by more than an order of magnitude, with little change taking place with the addition of further MCS-III. Figures 7, 8 and 9 are plots of G_p (the energy to propagate) versus weight per cent MCS-I in MCS-III. These were obtained from crack propagation studies as a function of temperature for samples formed at various temperatures. The data show: (1) Increasing the annealing temperature decreases G_p . (2) Increasing the crack propagation temperature reduces G_p . This effect has been reported previously and will be discussed later. (3) Except for the abrupt change in G_p with the addition of 20% MCS-III to MCS-I, $\log G_p$ is an approximately linear function of weight per cent MCS-I in MCS-III from 0 to 80%. At higher annealing temperatures the correlation is linear over the entire composition range. Therefore:

$$G_p \sim (\text{wt \% MCS-I})^n \quad (4)$$

Note that the slope of the G_p -% MCS-I correlation is ~ 1 except for data taken at 90°C, showing a similarity in the G_p dependence with the high shear viscosity molecular weight dependence observed in polymers, i.e.

$$\bar{M}_w = \sum_i w_i M_i \quad (5)$$

$$\begin{aligned} &= W(\text{MCS-I})M(\text{MCS-I}) \\ &\quad + W(\text{MCS-III})M(\text{MCS-III}) \\ &= \%(\text{MCS-I})W_T M(\text{MCS-I}) \\ &\quad + \%(\text{MCS-III})W_T M(\text{MCS-III}) \\ &= W_T (\%(\text{MCS-I})[M(\text{MCS-I}) - M(\text{MCS-III})] \\ &\quad + M(\text{MCS-III})) \end{aligned}$$

$$\therefore \bar{M}_w \sim \%(\text{MCS-I})$$

$$\therefore G_p \sim \bar{M}_w$$

where W_T is the total weight of the sample, % is the weight per cent of each molecular weight component, and in the high shear limit $\eta \sim M_w$ and in this case $\eta \sim \%(\text{MCS-I})$. In an earlier paper² we proposed a simple model in which flow occurred in the amorphous regions of MCS during crack propagation. Correlative data such as the above could indicate that such a proposition is correct and that molecular entanglements are important in the propagation process.

Since G_p does correlate with % MCS-I, it will not correlate with spherulitic radius (R) to the $-\frac{1}{2}$ power, as has been observed previously. This is especially true at higher annealing temperatures, where large changes in R are observed with composition changes.

Fracture morphology

The fracture morphology of the systems studied is not very different from those observed in earlier studies except that MCS-III is much more brittle and shows no plastic deformation zones. In earlier studies it was observed that a low-temperature quench and anneal (20°C) followed by tensile testing at 20°C provided fracture morphologies that exhibited plastic deformation. Examples of this are shown in Figure 10, where it is seen that large- or small-

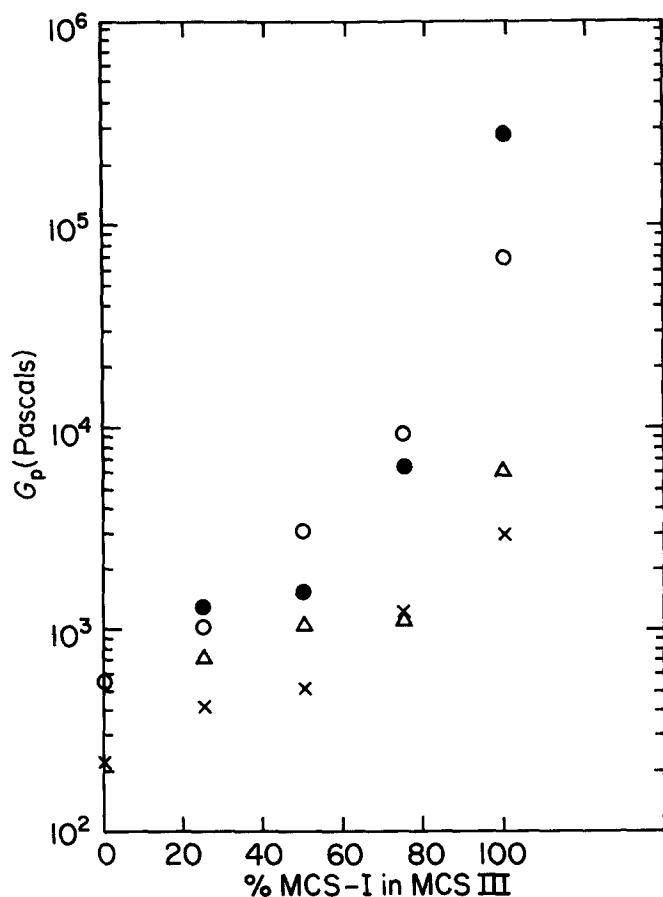


Figure 7 G_p as a function of weight per cent MCS-I in MCS-III. Samples formed at 23°C and propagated at the following temperatures: (●) 23°C, (○) 55°C, (△) 72°C, (×) 90°C

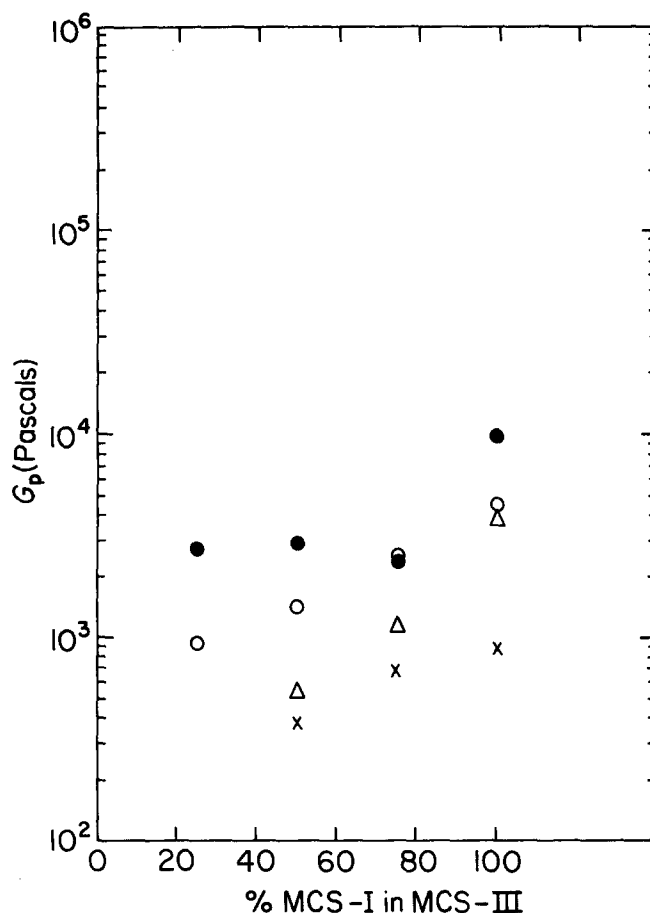


Figure 9 G_p as a function of weight per cent MCS-I in MCS-III. Samples formed at 85°C and propagated at the same temperatures as in Figure 7

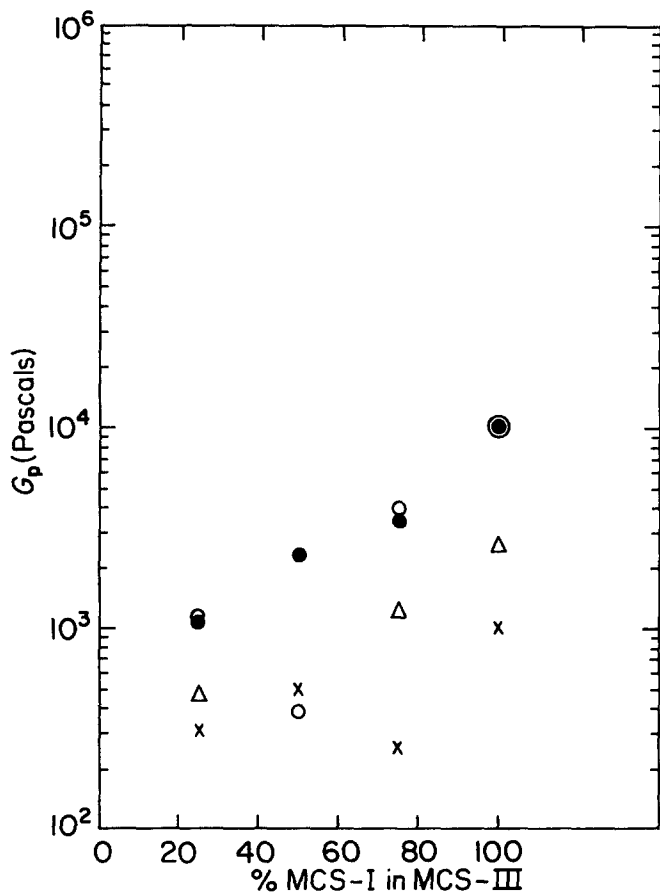


Figure 8 G_p as a function of weight per cent MCS-I in MCS-III. Samples formed at 55°C and propagated at the same temperatures as in Figure 7

scale plastic deformation can take place, depending on preparative and experimental conditions. Figure 10a shows trans-spherulitic fracture, with plastic deformation taking place only in certain band orientations of the spherulites. This deformation has previously been associated with crystal lamellae alignment^{1,14} in which the deformed areas have the chain axis aligned perpendicular to the stress direction. Figure 10b shows gross plastic deformation, yet the general outline of the spherulites can be seen. Samples formed and fractured at ambient display only plastic deformation^{1,2}. MCS-III fracture morphology, on the other hand, is totally brittle for all experiments performed. Samples of this morphology are shown in Figure 11. Both cases represent experimental conditions that would provide plastic deformation for higher-molecular weight MCS materials. Instead, MCS-III fractures trans-spherulitically with banding outlines being observed, but with no plastic deformation. The effect of increasing the MCS-I concentration in MCS-III at a given experimental condition is shown in Figure 12; Figure 11a can be included in this series. In these Figures, fracture proceeds from brittle uneven behaviour to even plastic deformation with increasing MCS-I content. This is observed with various degrees of deformation at all experimental conditions except when samples are formed and tested at 90°C; 90°C results are shown in Figures 13 and 14. At low magnification, the fracture morphologies of these samples appear very similar with interspherulitic failure dominant. High magnification of the trans-spherulitic fracture surfaces shows the 75% MCS-I sample fracturing

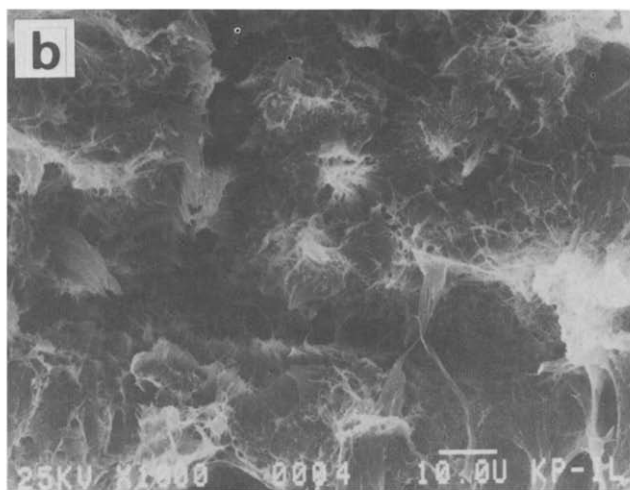
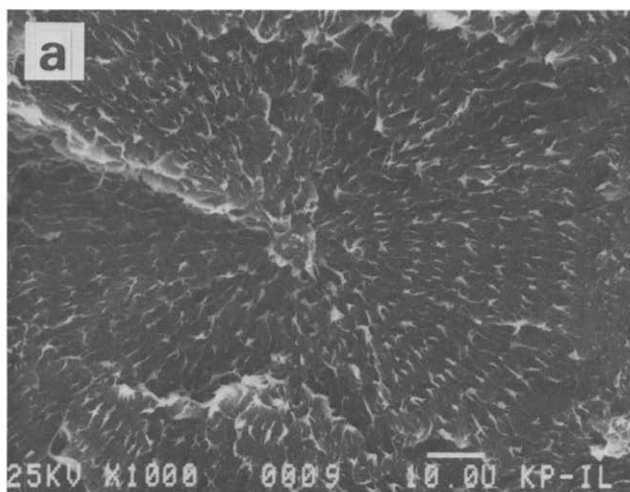


Figure 10 Fracture morphology of MCS-I: (a) quenched and annealed at 85°C, fractured at 55°C; (b) quenched and annealed at 23°C, fractured at 55°C

brittly but the 100% MCS-I sample exhibiting some plastic deformation due to band orientation.

Temperature dependence of fracture energy

Values of G_p as a function of forming and annealing conditions and blend composition are shown in Figures 15–17. The values plotted are log averages of all data taken. In some cases, particularly with samples of high MCS-III content, brittle fracture occurred during loading and tightening of the grips of the Instron tester, and G_p could not be measured. These trends are noted from the data: (1) With increased forming temperature the materials are weaker. (2) The materials become weaker with increased MCS-III content. (3) The materials show a stronger temperature dependence as the MCS-I content is increased. The first trend was observed previously and was associated with molecular-weight phase separation due to polymer crystallization^{1,3,4}. The second trend is also caused by crystallization and the fact that MCS-III is a weaker material than MCS-I. The third trend is interesting. Temperature-dependent data such as those in Figures 15–17 have originally been fit with equation (6)

$$G_p = \frac{1}{C_1} + \frac{1}{C_2 \exp(-E_a/RT)} \quad (6)$$

whose derivation was based on a local flow model for the amorphous material in MCS². It was shown that the activation energy was a function of forming temperature (decreasing with increasing forming temperature) and molecular weight. To fit experimental data, a series of reduced G_p versus T plots were made, and the activation energy was interpolated from the curves. If this technique is used for the data in Figures 15–17, the activation energies listed in Table 2 are obtained. Blanks in the Table indicate insufficient data to obtain the activation energies or errors in the fit so large that the activation energy is meaningless. The activation energies obtained for MCS-I are lower than those observed previously². We feel that this is due to a slight change in our sample preparation technique, which permitted the samples to cool slightly more slowly than previously. This would have caused nucleation and growth to occur at a higher temperature than expected² and thus would have lowered the energy needed to propagate a crack. This in turn would have lowered the apparent activation energy associated with the G_p temperature dependence. Of more importance is the decrease in E_a and the change to negative numbers with increasing MCS-III content! The apparent change in sign of E_a appears to correlate with a change in fracture mode in the mixtures. Thus, as the fracture becomes

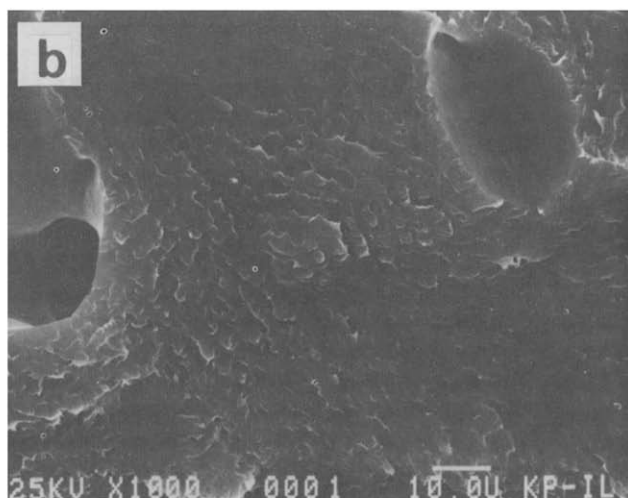
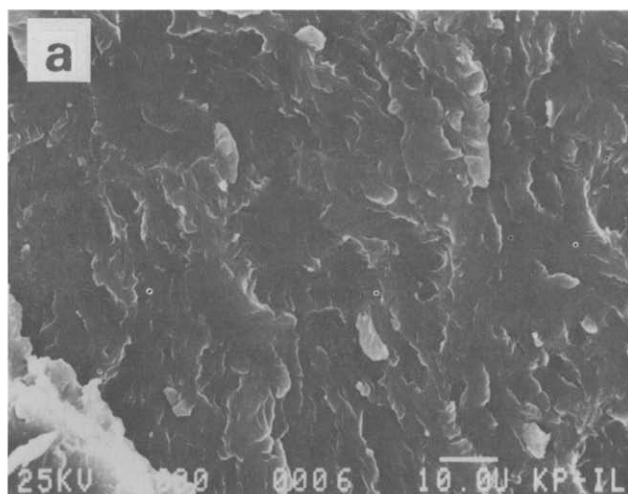


Figure 11 Fracture morphology of MCS-III: (a) quenched and annealed at 55°C, fractured at 23°C; (b) quenched and annealed at 40°C, fractured at 23°C

totally brittle (on the SEM scale that we are using) the apparent barrier becomes negative. How can these data be rationalized? One way is to assume that the activation energy is stress or strain dependent. Linear damage theory¹⁵ provides that the damage-accumulation rate can be written as an activated process:

$$R = A \exp(-\Delta H^+ - \sigma V^*)/kT$$

where ΔH^+ is an activated barrier for the disruptive process, σ is the applied stress and V^* is the activation volume for the material. Equations of this type are derived by assuming that fatigue deformation is a function only of a time-delayed response of applied stress. The activated process may include bond breakage, void formation, chain orientation, crystallinity changes and crystal phase changes. The presence of an applied stress

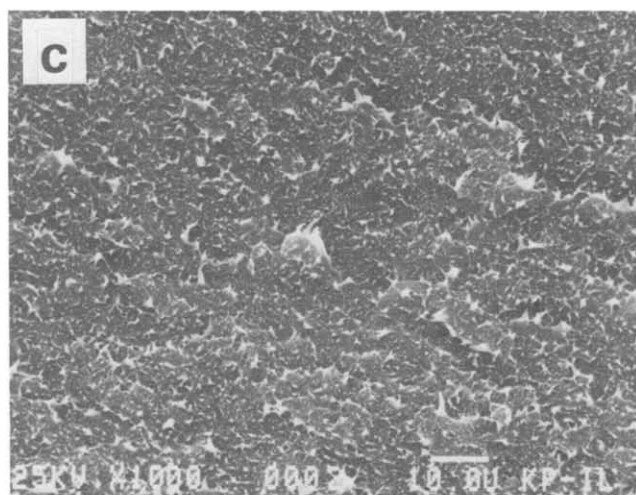
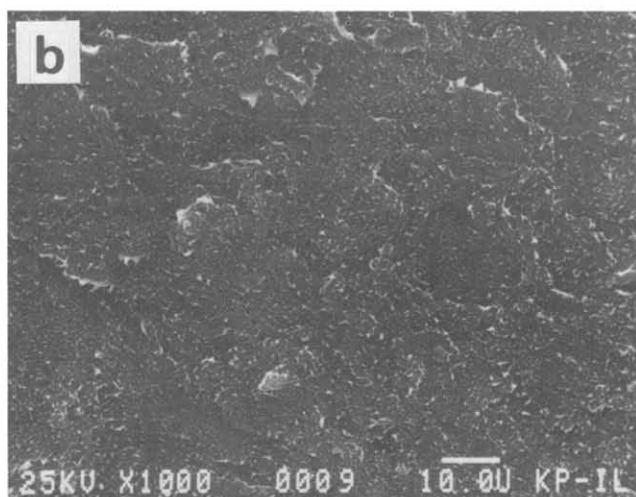
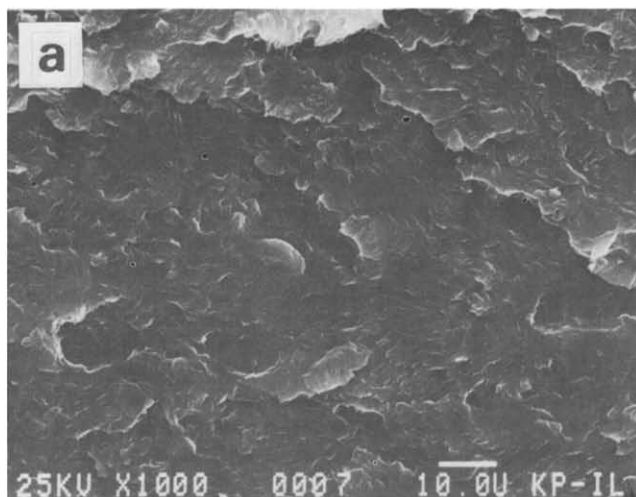


Figure 12 Fracture morphology of MCS-I/MCS-III blends. Samples quenched and annealed at 55°C, fractured as 23°C: (a) 25%, (b) 75%, (c) 100% MCS-I

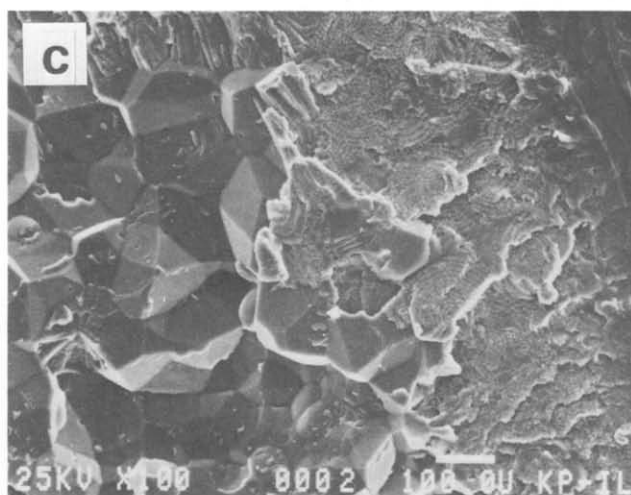
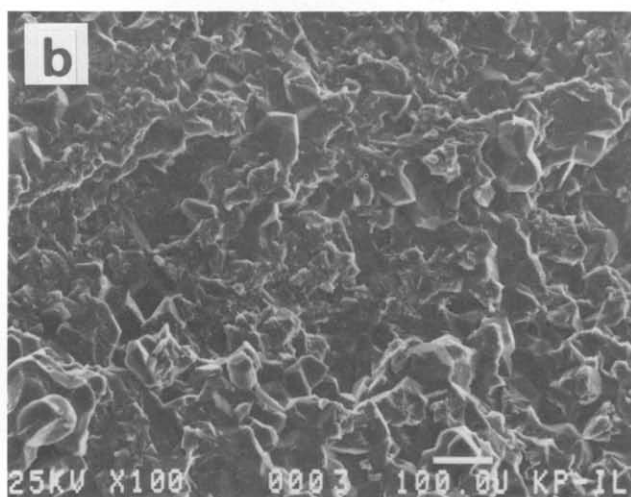
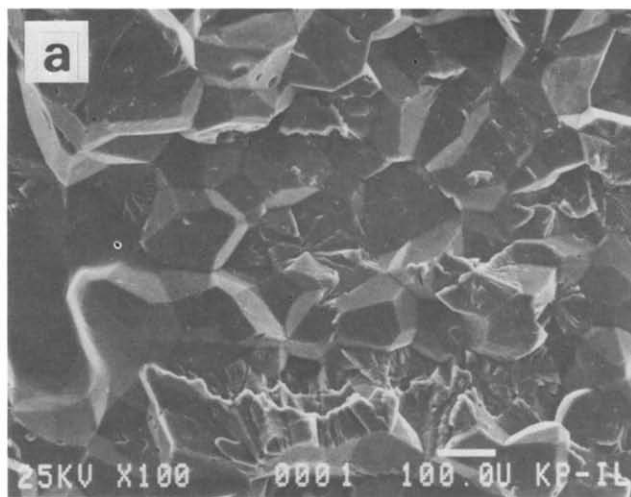


Figure 13 Fracture morphology of MCS-I/MCS-III blends. Samples quenched and annealed at 85°C, fractured at 90°C: (a) 50%, (b) 75%, (c) 100% MCS-I

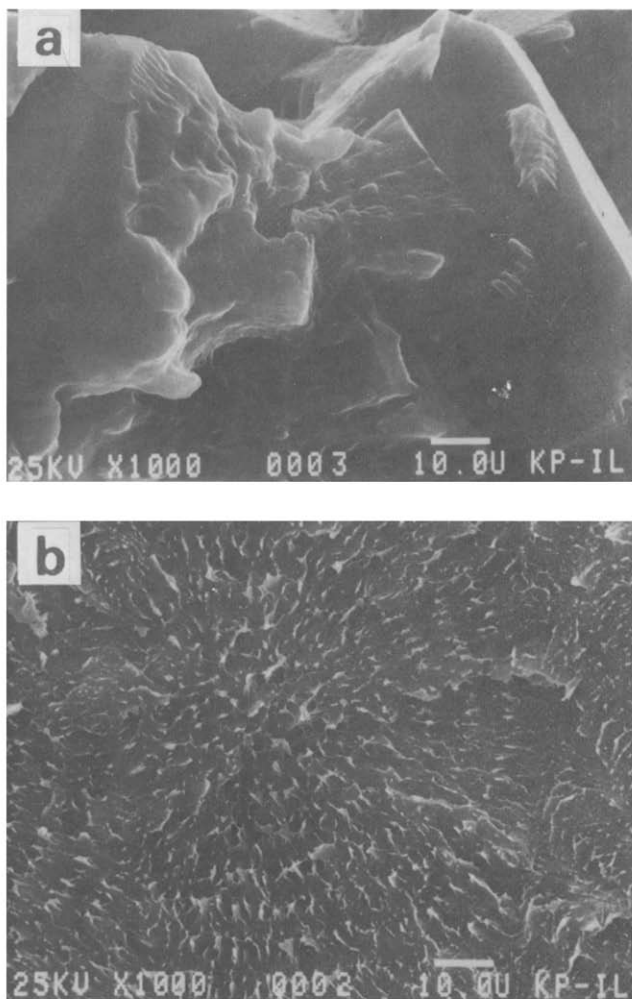


Figure 14 Fracture morphology of MCS-I/MCS-III blends. Samples quenched and annealed at 85°C, fractured at 90°C: (a) 75%, (b) 100% MCS-I

can skew the barrier and lower it. A change in sign of the barrier is, however, not physically meaningful, and equation (7) can be used only to describe barrier lowering. It would appear for these studies that either the assumptions made in deriving equation (6) no longer hold in the mixed systems or a blend with molecular weight distributions above and below entanglement cannot be treated the same as those above M_c . The data in Figures 15-17 also suggest that high-temperature annealing homogenizes the obtained activation energies to a common value.

ACKNOWLEDGEMENT

We thank J. R. Minter for helpful suggestions during the preparation of the manuscript.

REFERENCES

- 1 Pochan, J. M., Parsons, W. F. and Elman, J. F. *Polymer* 1984, **25**, 1031
- 2 Pochan, J. M., Elman, J. F. and Parsons, W. F. *Polymer* 1984, **25**, 1040
- 3 Bente, G. G. and Kniefel, R. M. *J. Am. Cer. Soc.* 1965, **48**, 570
- 4 Mandelkern, L., Fatou, J. S. and Howard, C. J. *J. Phys. Chem.* 1965, **69**, 956
- 5 Magill, J. H. *J. Polym. Sci., B* 1968, **6**, 853

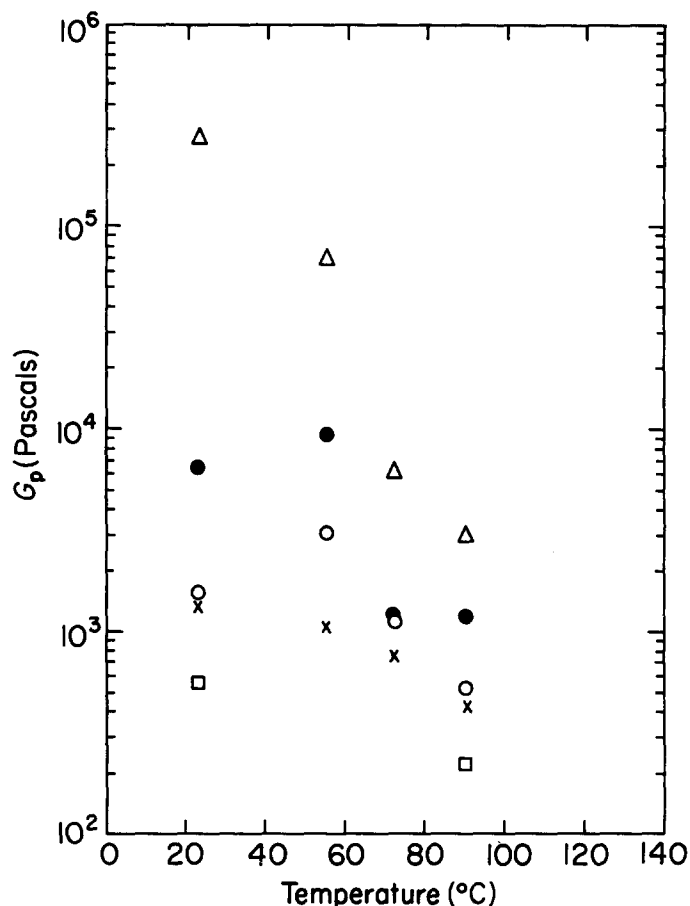


Figure 15 Energy to propagate versus temperature at propagation for MCS-I/MCS-III blends formed at 23°C (Δ) 100%, (●) 75%, (○) 50%, (×) 25% MCS-I

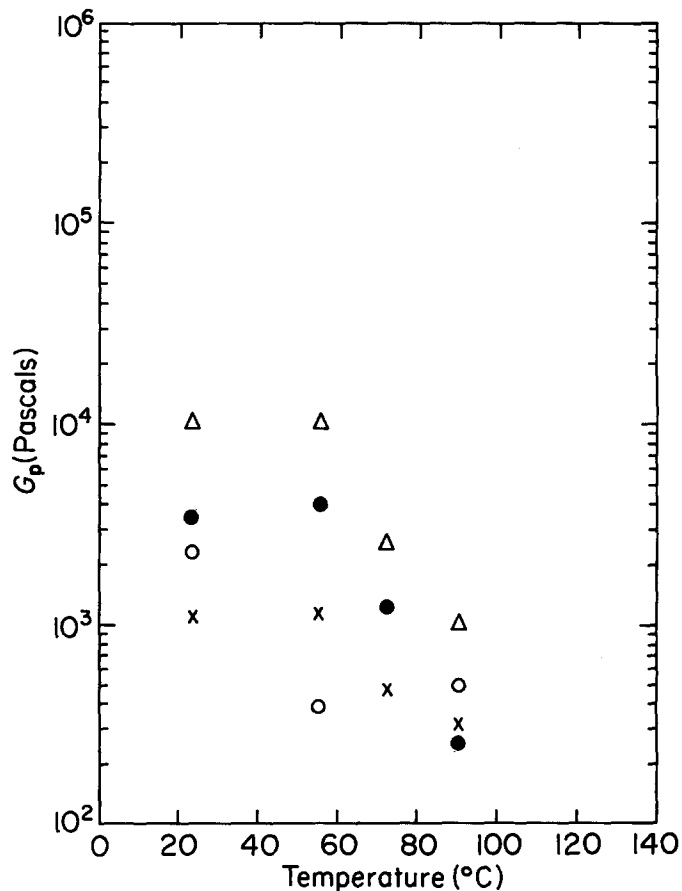


Figure 16 Energy to propagate versus temperature for MCS-I/MCS-III blends formed at 55°C; symbols as in Figure 15

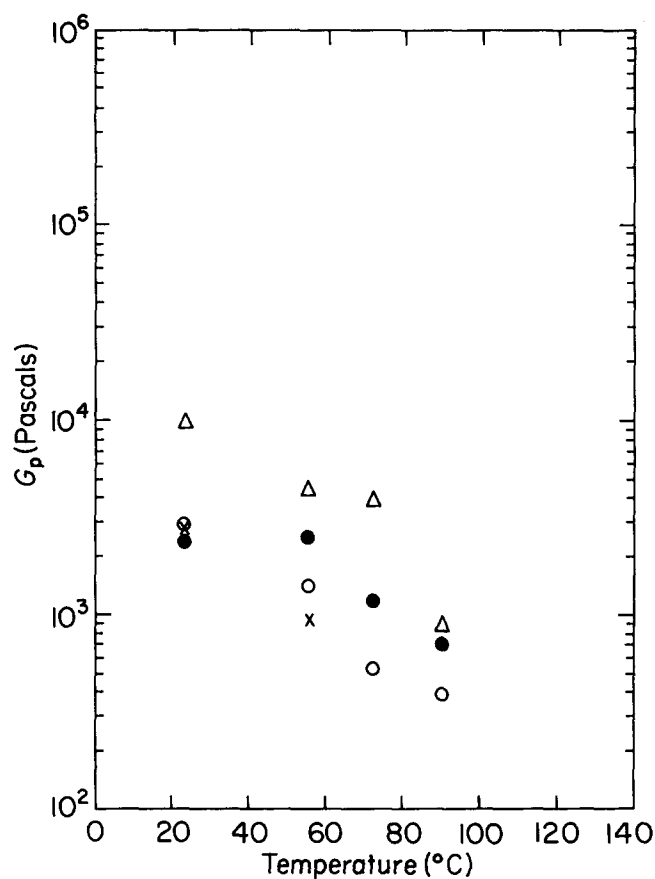


Figure 17 Energy to propagate versus temperature for MCS-I/MCS-III blends formed at 85°C; symbols as in Figure 15

Table 2 Activation energy from equation (6) for various blends of MCS-I in MCS-III at various forming temperatures

A Forming temperature = 23°C					
% MCS-I in MCS-III	0	25	50	75	100
E_a (kcal mol ⁻¹)	-	-10	-	-	10
B Forming temperature = 55°C					
% MCS-I in MCS-III	0	25	50	75	100
E_a (kcal mol ⁻¹)	-	-5	-	~0	5
C Forming temperature = 85°C					
% MCS-I in MCS-III	0	25	50	75	100
E_a (kcal mol ⁻¹)	-	-	0	-	~0

- 6 Mohajer, Y. and Wilkes, G. L. *J. Polym. Sci., Polym. Phys. Edn.* 1982, **20**, 457
- 7 Bobey, F. and Winslow, F. (Eds.) 'Macromolecules', Academic Press, New York, 1979, p. 326
- 8 Stein, R. S. and Rhodes, M. B. *J. Appl. Phys.* 1960, **31**, 1873
- 9 Moore, R. S. *J. Polym. Sci., A* 1965, **3**, 4093
- 10 Pochan, J. M. and Gibson, H. W. *J. Am. Chem. Soc.* 1969, **94**, 5573
- 11 Keith, H. D. and Padden, F. J. Jr. *J. Appl. Phys.* 1964, **38**, 4, 1286
- 12 Keith, H. D. and Padden, F. J. Jr. *J. Appl. Phys.* 1964, **38**, 4, 1270
- 13 Ref. 7, p. 347
- 14 Peterlin, A. 'Manmade Fibers: Science and Technology', John Wiley and Sons, New York, 1967, p. 283
- 15 Schultz, J. M. 'Treatise on Materials, Science and Technology, Vol. 10—Properties of Solid Polymeric Materials—Part B', Academic Press, New York, 1977, p. 628